NUMERICAL SIMULATION OF TURBULENT CHANNEL FLOW WITH PARTICLE ADHERED RIBLET SURFACES

Chikara Shimizu, Junichi Morita, Hiroya Mamori, Takeshi Miyazaki
Department of Mechanical and Intelligent Systems Engineering
The University of Electro-Communications
1-5-1, Chofugaoka, Chofu, Tokyo, 182-8585, Japan
mamori@uec.ac.jp

ABSTRACT

Numerical simulations of fully developed turbulent channel flows with riblet surfaces were carried out at the friction Reynolds number of 180. The influence of particles adhering to the triangular riblets on the drag reduction effect is investigated. The one-way coupling method is employed: the particles are affected by the fluid, but the fluid is not affected by the particles. The simulation consists of three steps: first, we calculate the adhesion position of the particles to riblets in the turbulent channel flow; second, the riblet shapes are changed based on the particle adhesion; third, we calculate the flow over the riblet with the adhered particles. As a result, most of the particles adhered near the upper edge of the riblets. Due to the particle adhesion on the riblets, the drag increases as compared with the case of the initial riblet of the riblet.

INTRODUCTION

With the development of industry, there is a growing interest in reducing energy consumption. Therefore, research on fluid drag reduction for energy reduction has been actively conducted. Turbulence control methods can be divided into active and passive control. Active control requires external energy, such as traveling wave control (Mamori et al. 2014). Passive control requires only initial processing, such as superhydrophobic surfaces (Fuaad and Arul Prakash 2019), polymers (Fujimura et al. 2017), and riblet surface.

The riblet surface means fine grooves on the wall, which is known to reduce turbulent friction drag, and many patterns of the riblet design have been studied. Choi et al. (1993) performed direct numerical simulations of a fully developed turbulent channel flow to investigate the two-dimensional riblet surface (referred to as the 2-D riblet, hereafter). They revealed that the lateral space between the riblet walls plays an important role, i.e., the drag reduction effect appears when the lateral spacing is smaller than the diameter of the vortical structure. Bechert et al. (1997) showed the blade-type riblets with very thin walls, and a maximum drag reduction was about 10%, where the lateral space between the riblets is $s^+ = 15$. In recent years, the three-dimensional riblet surface (the 3-D riblet) has been investigated. The 3-D riblet means that the riblet walls vary in the streamwise direction. Sasamori et al. (2014) made an experimental study to investigate the drag reduction effect by the sinusoidal riblet surface: it means that the lateral spacing between the riblet walls also varies periodically in the streamwise direction. They show that sinusoidal riblets provided a maximum drag reduction of 11.7%. In addition, the drag reduction effect is confirmed by the direct numerical simulation (Sasamori et al. 2017), and the vortical structure over the riblet surface is analyzed by using a dual-plane stereoscopic PIV (Mamori et al. 2019).

Accordingly, the 2-D and 3-D riblet surfaces are adequate for the drag reduction of the turbulent flow. However, from practical application, the riblet surface is employed for the outer flow where many small particles are floating and can adhere to the wall. The adhered particles may decrease the skin-friction drag reduction effect by the riblet, and therefore the robustness of the riblet against the particle adhering is essential.

In this study, we perform numerical simulations to investigate the effect of particles adhering to the riblets on the skin friction drag. The target of this simulation is a turbulent channel flow with a rectangular 2D-riblet surface. We perform one shot-simulation: first, we compute the turbulent flow with floating particles and obtain the distribution of the adhering particle; second, the riblet shape is changed due to the adhered particle; finally, we make the flow simulation again to estimate the variation of the drag reduction effect.

NUMERICAL SIMULATION

Numerical simulations of the particle-laden turbulent channel flow with the riblet are performed. The governing equations are continuity and Navier-Stokes equations for the incompressible flow, as

$$\frac{\partial u_i}{\partial x_i} = 0 \tag{1}$$

$$\frac{\partial u_i}{\partial t} + u_j \frac{\partial u_i}{\partial x_j} = -\frac{\partial p}{\partial x_i} + \frac{1}{\mathrm{Re}_\tau} \frac{\partial u_i^2}{\partial^2 x_j} \tag{2}$$

Here, u_i and x_i $(i = 1{\sim}3)$ are the velocity and the coordinates in the streamwise, wall-normal, and spanwise directions, respectively. In addition, t is time and p is the pressure. The coordinates x_i are interchangeably used as x, y, and z, the corresponding velocity components are used as u, v, and w, respectively. The friction Reynolds number defined by the wall friction velocity u_τ and the channel half-height δ is set to $\mathrm{Re}_\tau = 180$. This corresponds to the bulk Reynolds number of $\mathrm{Re}_b \approx 5600$ (based on the bulk velocity U_b and the channel half-height δ). The mean pressure gradient is kept

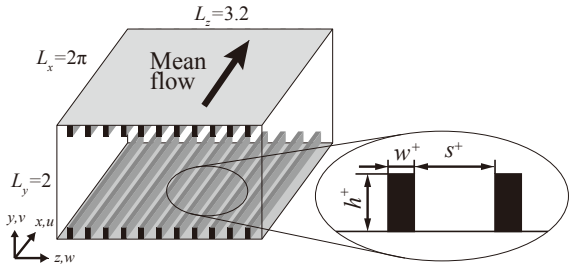

Figure 1. Schematic of the channel flow with the riblet surfaces.

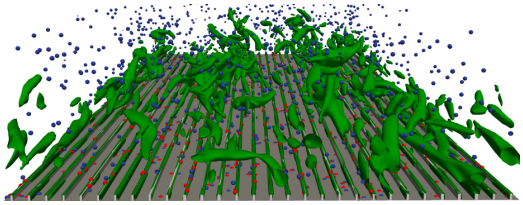

Figure 2. Schematic of the turbulent channel flow with the riblet surface together with the floating particles in the region near the lower wall.

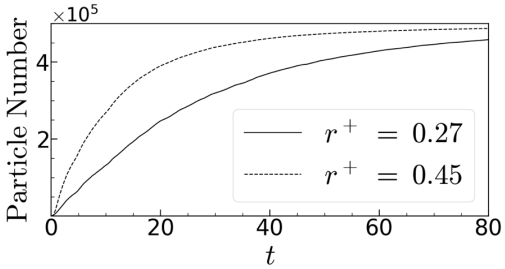

Figure 3. Time trace of number of adhering particles.

at constant. The velocity and pressure are defined on a staggered grid. The governing equations are discretized by the finite volume method.

Figure 1 shows the schematic of the channel flow with the riblet surface. The computational domain is set to $L_x \times L_y \times L_z = 2\pi \times 2 \times 3.2$, and the number of computational grids is set to $N_x \times N_y \times N_z = 128 \times 192 \times 512$. In boundary condition, the periodic condition is imposed in the streamwise and spanwise directions. The no-slip conditions are imposed on channel walls, and the riblets are represented by the immersed boundary method proposed by Kim et al. (2001).

The particle radius is set to 0.27 and 0.45 in the wall unit, and the density ratio of particles to fluid is set to 1.0×10^3. One-way coupling method is employed: the fluid affects the motion of the particles, but the particles do not affect the fluid.

The equation of motion of the particles considering the Stokes resistance is

$$m^* \frac{\partial \boldsymbol{v}_p^*}{\partial t^*} = -\frac{\pi}{2} \rho_f^* C_D r^{*2} |\boldsymbol{v}_r^*| \boldsymbol{v}_r^* \qquad (3)$$

Here, m is the mass of particles, ρ_f is fluid density, and r is particle radius. In addition, $\boldsymbol{v_r} = \boldsymbol{v_p} - \boldsymbol{v_f}$ is the relative velocity, $\boldsymbol{v_p}$ is particle velocity, and $\boldsymbol{v_f}$ is fluid velocity. The asterisk means dimensional quantities. The drag coefficient C_D is expected as,

$$C_D = \frac{24}{\mathrm{Re}_p} \qquad (\mathrm{Re}_p \le 1.0) \quad (4)$$

$$C_D = \frac{24}{\mathrm{Re}_p}\left(1 + 0.15\mathrm{Re}_p^{0.678}\right) \qquad (\mathrm{Re}_p > 1.0) \quad (5)$$

where, Re_p is the Reynolds number of particles based on the diameter and the relative velocity between the flow and particles. Particles are introduced only at the beginning of the calculation and no additional particles are introduced.

As shown in Fig. 1, the channel walls have a rectangular riblet surface. In the initial shape of the riblet surfaces (referred to as the initial riblet, hereafter), the height of the riblets, the width of the riblet, and the lateral spacing between the riblets are set to $h^+ = 7.5$, $w^+ = 3$, and $s^+ = 16.2$, respectively. Here, the superscript of the plus denotes the wall unit. Under these conditions, we installed 30 riblet walls on the upper and lower walls, respectively.

Next, we explain a numerical treatment of the particle adhered riblet surfaces. Although the adhered particles interact with the flow in the actual phenomenon, we employed single-shot calculation to reduce the computational cost. The procedure is as follows.

1. Particles are tracked as mass points and the adhesion distribution on the riblet surfaces is obtained at $0 \le t \le 80$. Here, the time origin $t = 0$ corresponds that the beginning of the simulation: the number of total added particles is set to $N_P = 5.0 \times 10^5$, the particles are randomly distributed in the fully developed turbulent channel flow with the riblet walls, and then we start to track the particles.
2. The adhesion distribution on the riblet and channel wall surface is computed. The height of the adhesion is obtained by the volume of adhered particles divided by the wetting area of the riblet and channel surface. Here, we make twofold assumptions: the adhesion distribution does not change as the number of adhesion particles N_P' increases; the particles uniformly adhere in the x-direction. Accordingly, we predict the riblet shape at $N_P' = 5.0 \times 10^5$ and 2.5×10^5.
3. The turbulent channel flow with the reshaped riblet surfaces is calculated, and we obtain the drag reduction rate and the flow statistics.

SAMPLE RESULTS

Figure 2 visualizes the turbulent flow in the region near the lower wall with the floating particles with $r^+ = 0.27$ at the beginning of the simulation. The riblet surface is clean. The riblet surface and floating particles are shown in gray and blue. The adhered particles are shown in red. The vortical structure is shown in green. In general, the riblet surfaces prevent the vortical structure from approaching the channel wall and the behaviour is observed.

Figure 3 shows the time variation of the total number of particles adhered to the channel and riblet walls. The number increases with the time advance. The number of adhered particles at $t = 80$ is approximately $N_P \approx 4.6 \times 10^5$ and 4.9×10^5 for $r^+ = 0.27$ and 0.45, respectively.

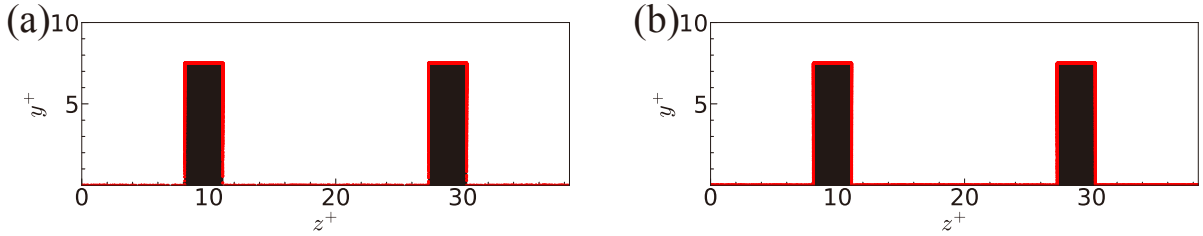

Figure 4. Distribution of the adhered particles on the riblet surface at t = 80: (a) r^+ = 0.27 and (b) r^+ = 0.45.

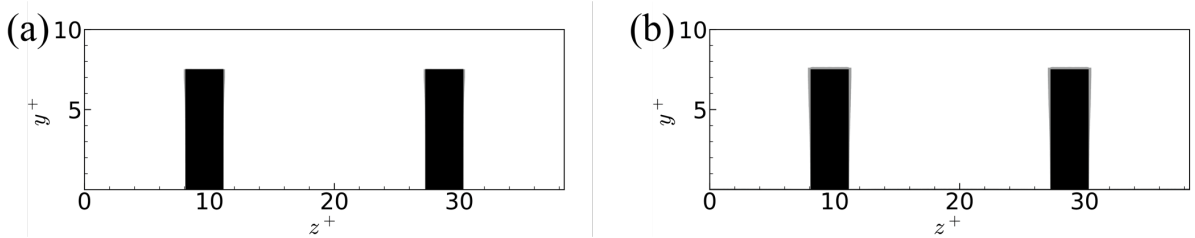

Figure 5. The particle adhered riblet for $N_P' = 5.0 \times 10^5$: (a) $r^+ = 0.27$ (Case 1) and (b) $r^+ = 0.45$ (Case 2).

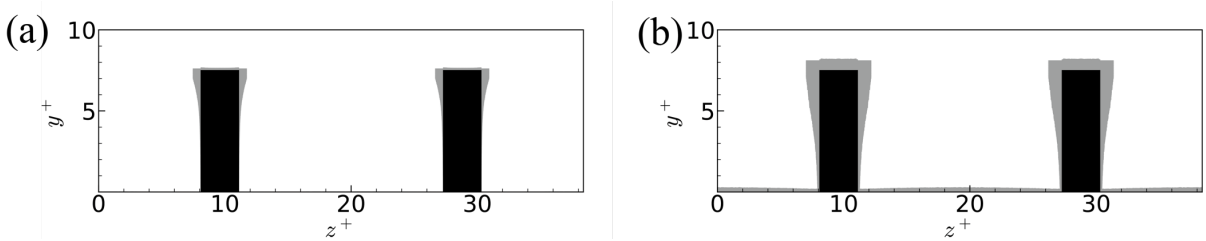

Figure 6. The particle adhered riblet for $N_P' = 2.5 \times 10^6$: (a) $r^+ = 0.27$ (Case 3) and (b) $r^+ = 0.45$ (Case 4).

Table 1. Parameter set for particle-adhered riblet shape.

	N_P	r^+
Case 1	5.0×10^5	0.27
Case 2	5.0×10^5	0.45
Case 3	2.5×10^6	0.27
Case 4	2.5×10^6	0.45

Table 2. The drag reduction rate by each case.

	R_D
initial riblet	4.24
Case 1	4.18
Case 2	3.29
Case 3	3.38
Case 4	2.09

Figure 4 shows the distribution of the adhered particles on the riblet surface at $t = 80$. The riblets are shown in black and adhered particles are shown in red. The figure is a perspective view i.e., all the adhered particle in the x-direction is shown on the y-z plane and the two riblet walls are shown as sample results. The particle size is $r^+ = 0.27$ in Fig. 4(a) and $r^+ = 0.45$ in Fig. 4(b). As shown in Fig. 4(a), the particles adhere to the whole of the riblet and channel surfaces. At the bottom of the riblet sidewalls, particles sparsely adhere. As shown in Fig. 4(b), particles adhere to the entire riblet and channel surfaces.

Next, we predict four particle-adhered riblet shapes, as shown in Table 1. Figure 5 shows particle-adhered riblet surfaces for $N_p' = 5.0 \times 10^5$. The initial riblet shape is colored by black and the predicted shape is colored by grey. As shown in Fig. 5, the change of the riblet shape is barely discernible, because the radius and number of adhered particles are small. Figure 6 shows the particle-adhered riblet surfaces for $N_p' = 2.5 \times 10^6$. As shown in Fig. 6(a), the adhesion layer covers the top edge of the riblet, results in the increase of the width of the top edge of the riblet. The adhesive layer covers the entire riblet and channel surfaces, and the riblets become a trapezoidal shape in Fig. 6(b). In addition, the particles are deposited on the channel wall surface. In all the cases, the amount of the adhesion increases at the ridges of the riblets. We suggest that particles are more likely to adhere there.

Finally, we perform numerical simulations of the turbulent flow over the predicted riblet surfaces. Since the pressure gradient is constant, an increase in the bulk velocity corresponds to an increase in the drag reduction rate. The drag reduction rate is shown in Table 2. The drag reduction rate is defined as

$$R_D = \frac{C_{f_0} - C_f}{C_{f_0}} \times 100 \qquad (6)$$

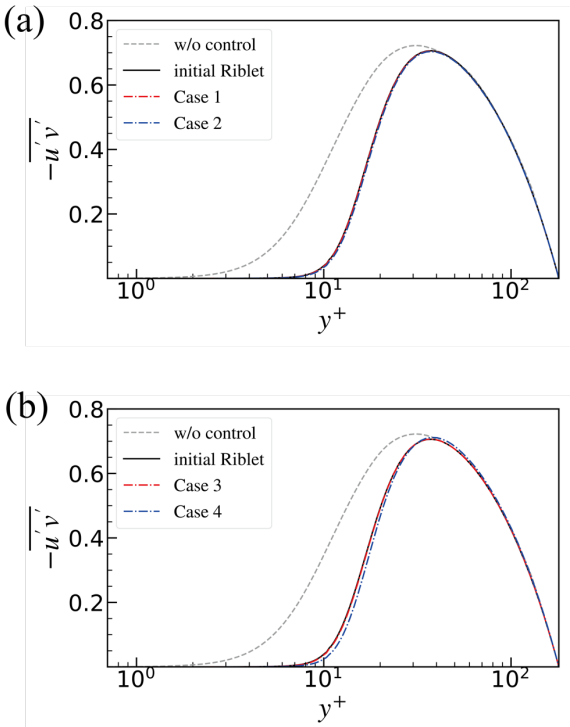

Figure 7. The Reynolds shear stress in Cases 1 and 2 (a) and Cases 3 and 4 (b).

Here, C_f is the coefficient of skin-friction drag, and the subscript of zero means the plane channel case (i.e., without the riblet and particle). In all the cases, the drag reduction ratio decreases due to the particle adhesion, the increase in the number of adhered particles and the volume of the particles. It is because the total volume of the adhered particles on the riblet increases as the number and radius of the particles increase.

The skin-friction coefficient C_f is decomposed as (Fukagata et al., 2002)

$$C_f = \frac{12}{\mathrm{Re_b}} + \frac{6}{U_b^2}\int_0^1 (1-y)(-\overline{u'v'})dy \qquad (7)$$

The first term is the laminar contribution. The second term is the contribution from the turbulence, which is the weighted integration of the Reynolds shear stress (referred to as the RSS, hereafter). Therefore, the skin-friction drag reduction corresponds to the decrease of the RSS.

Figure 7 shows the RSS at the center of the lateral spacing of the riblet walls. As compared to the clean channel flow (displayed by the w/o control), the RSS near the wall is reduced and the distribution shifts toward the center in the y-direction in the case of the initial riblet. Due to the adhesion of the particles, the RSS increased slightly and the drag reduction rate decreases.

CONCLUSION

We performed numerical simulations of the turbulent channel flow with the riblet and the floating particles. We investigated the effect of particle adhesion on the riblet shape and the drag reduction effect.

The particles tend to adhere to the ridge of the riblet surfaces. Based on it, we predict the riblet shape adhering to the particle. The drag reduction rate decreases as increase of the number of particles adhered and the Reynolds shear stress increases slightly.

REFERENCES

Bechert, D. W., Bruse, M., Hage, W., Van Der Hoeven, J. G. T., and Hoppe, G., 1997, "Experiments on drag-reducing surfaces and their optimization with an adjustable geometry.", *Journal of Fluid Mechanics*, Vol. 338, pp. 59-87.

Choi, H., Moin, P., and Kim, J., 1993, "Direct numerical simulation of turbulent flow over riblets," *Journal of Fluid Mechanics*, Vol. 255, pp. 503-539.

Fuaad P.A. and Arul Prakash, K., 2019, "Enhanced drag-reduction over superhydrophobic surfaces with sinusoidal textures: A DNS study.", *Computers and Fluids*, Vol. 181, pp. 208-223.

Fujimura, M., Iwamoto, K., Murata, A., Masuda, M., Ando, H., and Mamori, H., 2017, "Influence of length of polymer aggregation on turbulent friction drag reduction effect", *Journal of Fluid Science and Technology*, Vol. 12: 2.

Fukagata, K., Iwamoto, K., and Kasagi, N., 2002, "Contribution of Reynolds stress distribution to the skin friction in wall-bounded flows", *Physics of Fluids*, Vol. 14, pp. L73-L76.

Kim, J., Kim, D., and Choi, H., 2001, "An immersed-boundary finite-volume method for simulations of flow in complex geometries", *Journal of Computational Physics*, Vol. 171, pp. 132-150.

Mamori, H., Iwamoto, K., and Murata, A., 2014, "Effect of the parameters of traveling waves created by blowing and suction on the relaminarization phenomena in fully developed turbulent channel flow." *Physics of fluids*, Vol. 26: 015101.

Mamori, H., Yamaguchi, K., Sasamori, M., Iwamoto, K., and Murata, A., 2019, "Dual-plane stereoscopic PIV measurement of vortical structure in turbulent channel flow on sinusoidal riblet surface." *European Journal of Mechanics*, Vol. 74, pp. 99-110.

Sasamori, M., Iihama, O., Mamori, H. Iwamoto, K., and Murata, A., 2017, "Parametric study on a sinusoidal riblet for drag reduction by direct numerical simulation." *Flow Turbulence Combust*, Vol. 99, pp. 47–69.

Sasamori, M., Mamori, H., Iwamoto, K., and Murata, A., 2014, "Experimental study on drag reduction effect due to sinusoidal riblets channel flow," *Experiments in Fluids*, Vol. 55: 1828.